On Solutions for Two Waves with Periodic Coupling

By S. E. MILLER

(Manuscript received January 25, 1968)

An exact solution for the coupling effects between two waves with a particular complex periodic coupling function is presented; the particular coupling function gives the same wave interactions as constant coupling but at a translated value of differential phase constant. A transformation is given which permits known theory for constant coupling to be applied to the periodic coupling case.

Approximate solutions are given for periodically reversed coupling (sinusoidal or square wave) between two waves, and calculations are presented which indicate the solutions are valid for arbitrarily long coupling regions or arbitrarily large integrated coupling strengths. The region of validity for earlier perturbation theory is defined and proved to include the cases of interest for multimode circular electric waveguides.

I. INTRODUCTION

This paper describes some solutions for two waves with periodic coupling. Coupled waves have been important in a wide variety of communication devices: transmission lines, directional couplers, amplifiers, and in describing mode interchange phenomena generally.[1] Multimode transmission lines have been advantageously described through coupled wave equations, and a particular situation of importance exists in the circular electric waveguide.

As first shown by H. E. Rowe and W. D. Warters,[2] periodic straightness variations cause periodically reversed coupling from the circular electric wave to several other waves, and this interaction results in the most difficult tolerances on the fabrication and installation of the waveguide itself. Publications by H. E. Rowe and W. D. Warters have provided a comprehensive understanding of the fundamentals involved and have given explicit expressions based on perturbation theory for calculating the loss versus frequency varia-

tion resulting from such periodic mode conversion.[3] A subsequent publication by D. T. Young[4] has indicated how the approximate solution of Rowe and Warters may be transformed mathematically to show explicitly the way differential attenuation smooths out the mode-coupling effects on the loss versus frequency characteristic. Young's solution depends upon a valid perturbation solution. A discussion of the accuracy of the perturbation solution is given by H. E. Rowe;[5] when the differential attenuation is too small the perturbation solution breaks down and it is of interest to know exactly where and quantitatively how this occurs.

We show in this paper that a certain periodic coupling function has exactly the same effect on waves of unequal phase constant as uniform coupling between waves of identical phase constant. A transformation is given to allow the use of earlier theory for periodically coupled waves.

Also presented here is an approximate solution for the periodic coupling distribution sketched in Fig. 2 valid for any value of differential attenuation. It is true that known solutions for uniform coupling, as in Fig. 1, can be applied to Fig. 2 by simplying solving for the output values at $x = \lambda_m/2$ and using these as the input boundary conditions for the transmission region starting at $x = \lambda_m/2$. The resulting exact expression representing conditions at $x = \lambda_m$ can be expressed as a matrix and raised to the n^{th} power to represent the solution at $x = n\lambda_m$. We seek here a simpler form of expression in which the functional interrelations can be visualized without extensive numerical calculations.

II. EXACT SOLUTION FOR TWO PERIODICALLY COUPLED WAVES

We start with the following equations for two coupled waves:

$$\frac{d}{dz}E_1(z) = -\gamma_1 E_1 + c_{21}(z)E_2 \tag{1}$$

$$\frac{d}{dz}E_2(z) = c_{12}(z)E_1 - \gamma_2 E_2 \tag{2}$$

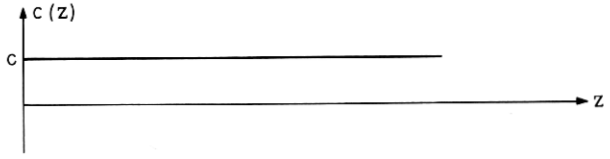

Fig. 1 — Constant coupling.

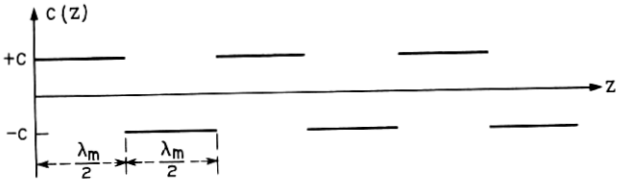

Fig. 2 — Square-wave coupling.

in which γ_1 and γ_2 are the complex propagation constants and c_{12} and c_{21} are coupling functions. Appendix A shows that the coupling functions

$$c_{21} = jc_p \exp(jk_c z) = jc_p[\cos k_c z + j \sin k_c z] \tag{3}$$

and

$$c_{12} = jc_p \exp(-jk_c z) = jc_p[\cos k_c z - j \sin k_c z] \tag{4}$$

give the same solutions previously found[6] for $k_c = 0$ provided that

$$k_c = (\beta_2 - \beta_1) = \Delta\beta \tag{5}$$

where c_p is a constant and

$$\gamma_m = \alpha_m + j\beta_m . \tag{6}$$

When (5) holds, complete transfer of power between waves can occur. When (5) does not hold, the resulting wave interactions can be calculated using previously developed theory for $k_c = 0$ and substituting ΔB for $\Delta\beta$ in the $k_c = 0$ solutions, where

$$\Delta B = \Delta\beta + k_c \tag{7}$$

III. PHYSICAL REALIZATION OF IDEAL PERIODICALLY COUPLED WAVES

We describe here a physical realization of waves coupled according to equations (3) and (4), and cite an advantage in mode selective directional couplers.

Figure 3 shows a mode-selective coupler between $TE_{10}^{\square}$ of rectangular guide and TE_{01}° of round guide. The thin dielectric lining is used to break the $TE_{01}^{\circ} - TM_{11}^{\circ}$ degeneracy. The longitudinal magnetic intensity h_z° of the TE_{01}° wave is coupled to the longitudinal magnetic intensity $h_z^{\square}$ of $TE_{10}^{\square}$ in the off-axis longitudinal slots and is also coupled to the transverse magnetic intensity $h_t^{\square}$ of $TE_{10}^{\square}$ in the 45° slots on-axis. In each case the magnitude of the coupling is set by the length and width of the slot.

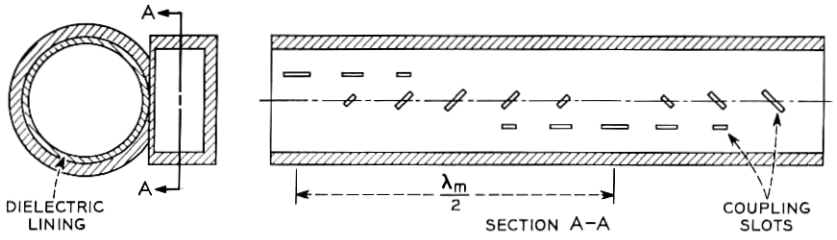

Fig. 3 — $TE^{\square}_{10}$-TE°_{01} coupler using unequal phase constants in the rectangular and round waveguides.

The phase reversal of the longitudinal $h_z^{\square}$ coupling is accomplished by reversing the slot position relative to the centerline, and the phase reversal of the transverse $h_t^{\square}$ coupling is accomplished by reversing the slant angle of the slot. One set of slots represents the sine term. It is not necessary that any particular fraction of λ_m be used in a coupler, since the coupling is always in the same phase relative to the desired waves in the two guides. To accomplish the desired mode selectivity the $\Delta\beta$ between the $TE_{10}^{\square}$ and TE_{01}° waves is made equal to $k_c = 2\pi/\lambda_m$ as in equation (5).

An advantage of a coupler of this form, compared with one in which constant coupling is used with $\Delta\beta = 0$, is that the waveguides can have the standard dimensions set by other considerations.

Other illustrations of useful coupling between waves of unequal phase constants will be given in another paper which the author is preparing.

IV. SQUARE-WAVE OR SINUSOIDAL COUPLING

We present here the results of Appendices B and C which discuss approximate solutions for the cases in which the coupling is a square wave as in Fig. 2, or the corresponding sinusoidal

$$c(z) = \sin(2\pi z/\lambda_m). \tag{8}$$

Both solutions are expressed in the form and notation of a previous publication[6] giving the solution when the coupling is constant, and the boundary conditions $E_1(0) = 1.0$ and $E_2(0) = 0$ are impressed:

$$E_1(z) = e^{-\gamma_{12}z}\{Ae^{r_{12}z} + Be^{r_{22}z}\} \tag{9}$$

$$E_2(z) = \frac{e^{-\gamma_{12}z}}{2\sqrt{\quad}}\{e^{r_{12}z} - e^{r_{22}z}\} \tag{10}$$

in which

$$A = \left[\frac{1}{2} - \frac{1}{2}\frac{\left(\frac{\Delta\beta_*}{2c_*}\right) - i\left(\frac{\Delta\alpha}{2c_*}\right)}{\sqrt{\ }}\right] \tag{11}$$

$$B = \left[\frac{1}{2} + \frac{1}{2}\frac{\left(\frac{\Delta\beta_*}{2c_*}\right) - i\left(\frac{\Delta\alpha}{2c_*}\right)}{\sqrt{\ }}\right] \tag{12}$$

$$r_{\substack{1\\2}} = \frac{\Delta\gamma_*}{2} \pm ic_*\sqrt{\ } \tag{13}*$$

$$\sqrt{\ } = \sqrt{1 + \left(\frac{\Delta\beta_*}{2c^*}\right)^2 - \left(\frac{\Delta\alpha}{2c_*}\right)^2 - i2\left(\frac{\Delta\beta_*}{2c^*}\right)\left(\frac{\Delta\alpha}{2c^*}\right)} \tag{14}$$

$$\Delta\alpha = \alpha_1 - \alpha_2$$

$$\Delta\gamma_* = \Delta\alpha + i\Delta\beta. \ .$$

The wave interactions are described by the above equations provided the following values of c_* and $\Delta\beta_*$ given in Table I are used.

TABLE I — VALUES OF c_* AND $\Delta\beta_*$

Coupling function (see Fig. 2)	c_*	$\Delta\beta_*$
Constant $= c$	c	$\Delta\beta = (\beta_1 - \beta_2)$
Square-wave of magnitude c and period λ_m	$\frac{2}{\pi}c$	$\Delta\beta - \frac{2\pi}{\lambda_m}\sqrt{1 - \left(\frac{c\lambda_m}{\pi}\right)^2}$
$c \sin\left(\frac{2\pi z}{\lambda_m}\right)$	$\frac{c}{2}$	$\Delta\beta - \frac{2\pi}{\lambda_m}$

These solutions, equations (9) and (10), have been obtained in Appendix B by relating the rate of transfer of power (that is, transfer over a short length interval) for the periodically reversed coupling to that for constant coupling, and noting the effective value of coupling c_* and effective differential phase constant $\Delta\beta_*$. The solutions are correct for z equal to an integral multiple of $\lambda_m/2$, and may be in error by less than approximately $0.2c\lambda_m/\pi$ at intermediate values of z.

There probably should be a correction factor in $\Delta\beta_*$ for sinusoidal

* r_1 corresponds to the + sign and r_2 corresponds to the — sign.

coupling similar to the radical shown in Table I for the square wave coupling; the work done thus far has not defined what it should be, but for small $c\lambda_m$ the radical is negligible for most purposes.

The values of $\Delta\beta_*$ in Table I bear marked resemblance to equation (7); however, because the simple sinusoid or square wave coupling phase is two-valued (versus z) instead of continually progressing (equations 3 and 4) to provide coupling continuously in step with the phase changes of waves 1 and 2, there are local maxima* in coupling effects at other values of $\Delta\beta$ for sinusoidal or square wave coupling. Appendix B shows that the wave interaction effects are properly described for square wave coupling in the regions near

$$\Delta\beta\lambda_m = 2\pi p \qquad p = 1, 3, 5, \cdots \tag{15}$$

by the transformations

$$\Delta\beta_* = \Delta\beta - p\frac{2\pi}{\lambda_m}\sqrt{1 - \left(\frac{c\lambda_m}{p\pi}\right)^2} \tag{16}$$

$$c_* = \frac{2c}{p\pi}. \tag{17}$$

Because c_* drops off rapidly with increasing p the corresponding wave interaction effects drop off also.

4.1 *Numerical Comparison of Approximate and Exact Solutions*

A few calculations have been made to find quantitatively the error resulting from the approximations made in equations (9) and (10) for coupling as in Fig. 2. An "exact" solution is obtained by using exact uniform coupling theory on each interval of 0.5 λ_m, the output of one interval being taken as the input to the next interval.

We take first the simplest case,

$$\Delta\alpha = 0.$$

Then equation (9) becomes

$$E_1\,|_{\Delta\alpha=0} = \exp\left[i\frac{(\beta_1 + \beta_2)_z}{2}\right] \cdot \left\{\cos\left[\sqrt{-\frac{2}{\pi}cz}\right] - i\frac{\left(\frac{\Delta\beta_*}{4c/\pi}\right)}{\sqrt{\quad}}\sin\left[\sqrt{-\frac{2}{\pi}cz}\right]\right\} \tag{18}$$

* Rowe and Warters noted this in their work recorded in Ref. 3.

$$E_2 \mid_{\Delta\alpha=0} = -\exp\left[i\frac{(\beta_1+\beta_2)z}{2}\right]\left\{\frac{ic}{\sqrt{\;}}\sin\left[\sqrt{\;}\frac{2}{\pi}cz\right]\right\} \tag{19}$$

in which

$$\sqrt{\;} = \sqrt{\left(\frac{\Delta\beta_*}{4c/\pi}\right)^2 + 1} \tag{20}$$

and $\Delta\beta_*$ is as given in Table I for square wave coupling. We notice in passing that for $\Delta\beta_* = 0$

$$E_1 = \cos\left(\frac{2}{\pi}cz\right) \tag{21}$$

$$E_2 = i\sin\left(\frac{2}{\pi}cz\right) \tag{22}$$

and the power exchanges completely back and forth between the two waves as a function of z; this is of course identical to the behavior in uniformly coupled waves, but with a modified period given by the $2/\pi$ factor.

We take for the first numerical comparison the condition

$$\frac{2}{\pi}cz = \frac{\pi}{2}$$

so that at $\Delta\beta_* = 0$, $E_1 = 0$ and $\mid E_2 \mid = 1.0$. The additional specific numbers used are

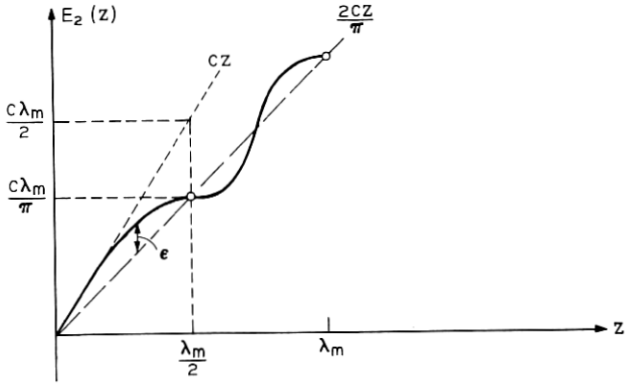

Fig. 4 — Undriven-wave amplitude versus distance for lowest order square-wave coupling.

$$\lambda_m = 2 \text{ feet}$$

$$z = 1000 \text{ feet}$$

$$c = 2.46740 \times 10^{-3} \text{ ft}^{-1}.$$

Fig. 6 shows a plot of the loss 20 log $| E_1 |$ (labelled $| \Delta\alpha/c | = 0$) versus $\Delta\beta_*\lambda_m/2$ and Table II shows the comparison of the exact versus approximate calculations, the latter obtained from equation (9) and associated expressions. It may be kept in mind that $\Delta\beta$ and $\Delta\beta_*$ are inversely proportional to frequency in many cases of interest, so that Fig. 6 is a loss versus frequency plot associated with a particular periodic coupling component. The radical in the expression for $\Delta\beta_*$ was ignored in the comparison of Table II and this might account for the consistent positive difference (approximate—exact) for $\Delta\beta\lambda_m/2$ greater than π. Aside from the pole at $\Delta\beta\lambda_m/2 = \pi$, the two calculations agree to better than 1 percent in dB even when the loss is a few tenths of a dB.

Figs. 6 and 7 and Tables III, IV, and V show similar comparisons for $\Delta\alpha = -|c|$, $\Delta\alpha = -5|c|$, and $\Delta\alpha = -50|c|$. Excellent agreement is obtained in all cases.

Table VI shows a comparison of the phase angle on E_1, computed by the two approaches. For the points shown and for the other points (not shown) corresponding to the amplitude values of Tables II and V the agreement is excellent. Fig. 8 shows a plot of the phase, where odd symmetry about $\Delta\beta_* = 0$ is understood.

A check has also been made on the accuracy of equation (9) in the region near $\Delta\beta\lambda_m = 6\pi$, corresponding to $p = 3$ in equations (15) through (17). The same parameters were used as in the calculations for Figs. 6 and 7. The results are plotted in Figs. 9 and 10 which represent *both* the approximate calculation from equation (9) and the exact calculation. The differences are on the same order as given in Table II, and are too small to show in the figures. Figures 9 and 10 may be compared directly with Figs. 6 and 7 to see the "third harmonic" loss (labelled E_1^3 in Figs. 9 and 10) in relation to the "fundamental" loss, Figs. 6 and 7.

4.2 *Interpretation and Further Simplification*

Consider first the shape of the loss versus $\Delta\beta_*$ (equivalent to loss versus frequency) curves. In the limit

$$\left| \frac{\Delta\alpha}{c} \right| \gg 1 \tag{23}$$

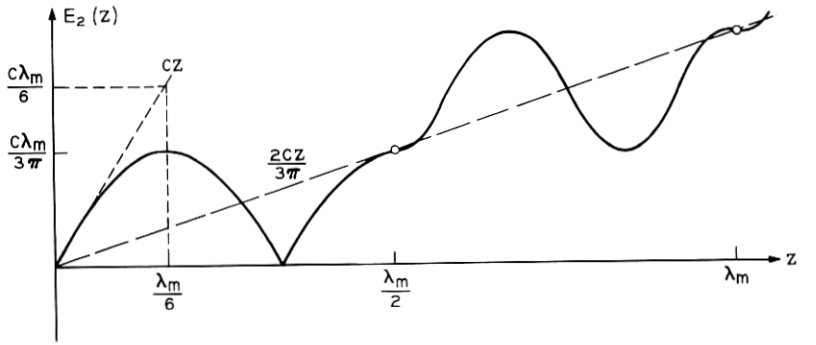

Fig. 5 — Undriven-wave amplitude versus distance for "third harmonic" in square-wave coupling.

TABLE II — EXACT AND APPROXIMATE CALCULATIONS OF E_1 FOR $|\Delta\alpha/c| = 0$

$\Delta\beta\left(\frac{\lambda_m}{2}\right)$	20 log $\lvert E_1 \rvert$		Approximate −exact
	Approximate	Exact	
$\pi - 0.0157079$	− 0.1662db	− 0.1680db	+ 0.0018db
$\pi - 0.01413716$	− 0.1389	− 0.1403	+ 0.0014
$\pi - 0.01256637$	− 0.0094	− 0.0096	+ 0.0002
$\pi - 0.01099557$	− 0.0951	− 0.0960	+ 0.0009
$\pi - 0.009424777$	− 0.4270	− 0.4300	+ 0.0030
$\pi - 0.0078539816$	− 0.4973	− 0.4999	+ 0.0026
$\pi - 0.006283185$	− 0.1156	− 0.1161	+ 0.0005
$\pi - 0.0047123889$	− 0.1260	− 0.1267	+ 0.0007
$\pi - 0.00314159264$	− 1.6530	− 1.6582	+ 0.0052
$\pi - 0.0015707963$	− 6.4362	− 6.4540	+ 0.0178
π	− 122.73	− 58.54	
$\pi + 0.0015707963$	− 6.4362	− 6.4184	− 0.0178
$\pi + 0.00314159264$	− 1.6530	− 1.6481	− 0.0049
$\pi + 0.0047123889$	− 0.1260	− 0.1255	− 0.0005
$\pi + 0.006283185$	− 0.1156	− 0.1154	− 0.0002
$\pi + 0.0078539816$	− 0.4973	− 0.4949	− 0.0024
$\pi + 0.00942477$	− 0.4270	− 0.4243	− 0.0027
$\pi + 0.01099557$	− 0.0951	− 0.0944	− 0.0007
$\pi + 0.01256637$	− 0.0094	− 0.00964	+ 0.0002
$\pi + 0.01413716$	− 0.1389	− 0.1378	− 0.0011
$\pi + 0.0157079$	− 0.1662	− 0.1646	− 0.0016

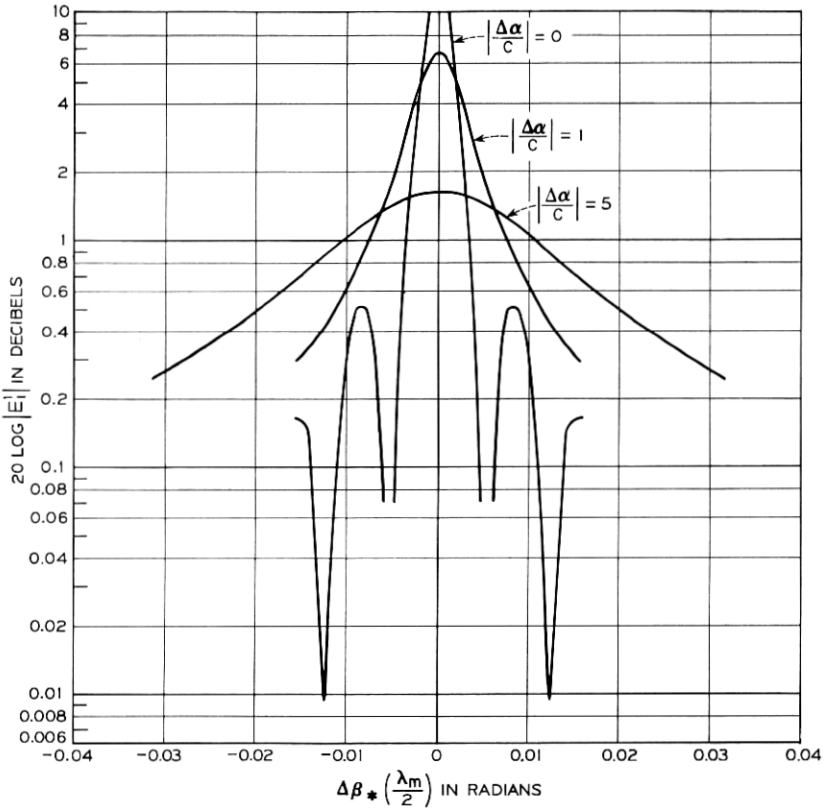

Fig. 6 — Driven-wave loss versus $\Delta\beta_*$ near $\Delta\beta\lambda_m = 2\pi$ (fundamental) for $|\Delta\alpha/c| = 0,1,5$.

earlier perturbation theory[4] has shown that the fractional frequency interval between half-height points on the loss curve is

$$\frac{\Delta f}{f} = \frac{\Delta\beta_{*\frac{1}{2}}}{\Delta\beta} = 2\left|\frac{\Delta\alpha}{\Delta\beta}\right| \tag{24}$$

or

$$\Delta\beta_{*\frac{1}{2}} = 2\,|\,\Delta\alpha\,|. \tag{25}$$

Table VII shows a comparison between that limiting value and the true value for the numerical cases above, including $|\Delta\alpha/c|$ from one to 50. Even at $|\Delta\alpha/c| = 1$ there is only a 30 per cent error.

Consider the limiting case $\Delta\alpha = 0$. Then

$$E_1 = [1 - (E_2)^2]^{\frac{1}{2}} \tag{26}$$

and nulls in the loss curve occur when equation (19) representing E_2 is zero. This gives

$$\Delta\beta_* \,|_{\text{loss null}} = \frac{4c}{\pi}\sqrt{\left(\frac{\pi^2}{2cz}\right)^2 - 1}. \tag{27}$$

When we also have the perturbation condition, $cz \ll 1$, equation (27)

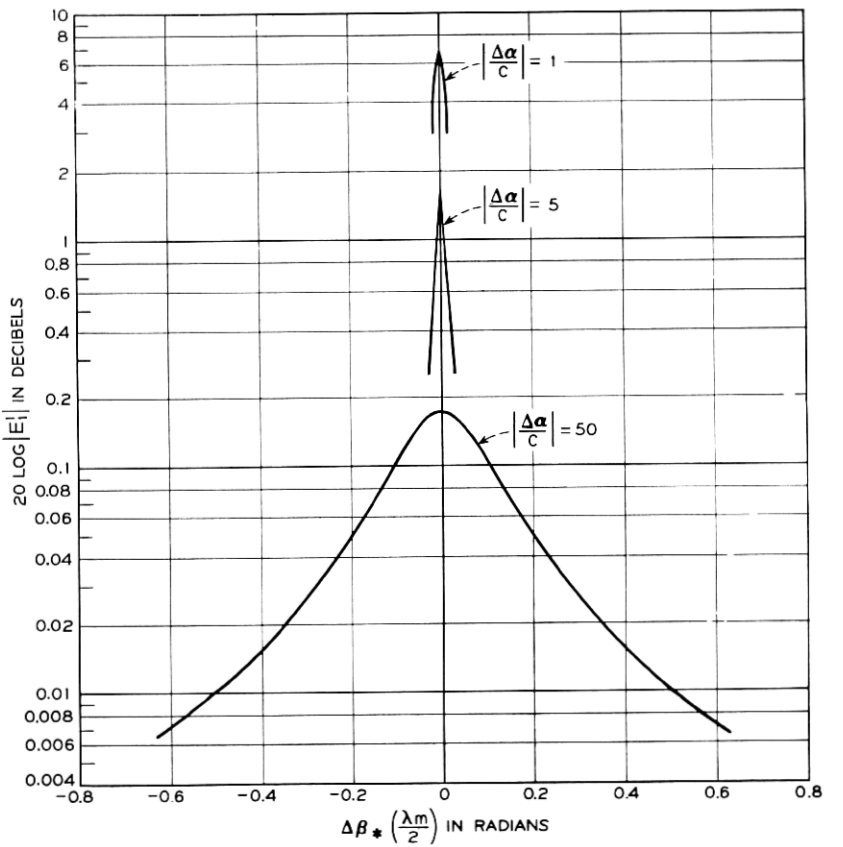

Fig. 7 — Driven-wave loss versus $\Delta\beta_*$ near $\Delta\beta\lambda_m = 2\pi$ (fundamental) for $|\Delta\alpha/c| = 1,5,50$.

becomes

$$\Delta\beta_* \mid_{\text{null}} \cong \frac{2\pi}{z} \tag{28}$$

which agrees with previously known perturbation theory.[3] For this

TABLE III — EXACT AND APPROXIMATE CALCULATIONS OF E_1 FOR $\mid \Delta\alpha/c \mid = 1$

$\Delta\beta\left(\frac{\lambda_m}{2}\right)$	20 log $\mid E_1 \mid$		Approximate −exact
	Approximate	Exact	
$\pi - 0.0157079$	− 0.2898	− 0.2910db	+ 0.0012db
$\pi - 0.01413716$	− 0.3438	− 0.3450	+ 0.0012
$\pi - 0.01256637$	− 0.4152	− 0.4164	+ 0.0012
$\pi - 0.01099557$	− 0.5452	− 0.5440	+ 0.0012
$\pi - 0.009424777$	− 0.7300	− 0.7319	+ 0.0019
$\pi - 0.0078539816$	− 0.9601	− 0.9620	+ 0.0019
$\pi - 0.006283185$	− 1.3106	− 1.3126	+ 0.0020
$\pi - 0.0047123889$	− 2.0216	− 2.0243	+ 0.0027
$\pi - 0.00314159264$	− 3.3781	− 3.3823	+ 0.0042
$\pi - 0.0015707963$	− 5.3475	− 5.3523	+ 0.0048
π	− 6.5701	− 6.5705	+ 0.0004
$\pi + 0.0015707963$	− 5.3475	− 5.3434	+ 0.0041
$\pi + 0.00314159264$	− 3.3781	− 3.3746	− 0.0035
$\pi + 0.0047123889$	− 2.0216	− 2.0194	− 0.0022
$\pi + 0.006283185$	− 1.3106	− 1.3092	− 0.0014
$\pi + 0.0078539816$	− 0.9601	− 0.9588	− 0.0013
$\pi + 0.00942477$	− 0.7300	− 0.7289	− 0.0011
$\pi + 0.01099557$	− 0.5425	− 0.5416	− 0.0009
$\pi + 0.01256637$	− 0.4152	− 0.4146	− 0.0006
$\pi + 0.01413716$	− 0.3438	− 0.3430	− 0.0008
$\pi + 0.0157079$	− 0.2898	− 0.2892	− 0.0006

TABLE IV — EXACT AND APPROXIMATE CALCULATIONS OF E_1 FOR $\mid \Delta\alpha/c \mid = 5$

$\Delta\beta\left(\frac{\lambda_m}{2}\right)$	20 $\log_{10} \mid E_1 \mid$		Approximate −exact
	Approximate	Exact	
$\pi - 0.0314159262$	− 0.2446db	− 0.2452db	+ 0.0006db
$\pi - 0.01884955$	− 0.5337	− 0.5344	+ 0.0007
π	− 1.6195	− 1.6197	+ 0.0002
$\pi + 0.01884955$	− 0.5337	− 0.5344	+ 0.0007
$\pi + 0.0314159$	− 0.2446	− 0.2445	+ 0.0001

TABLE V — EXACT AND APPROXIMATE CALCULATIONS OF E_1 FOR $|\Delta\alpha/c| = 50$

$\Delta\beta\left(\frac{\lambda_m}{2}\right)$	$20 \log_{10} \lvert E_1 \rvert$		Approximate −exact
	Approximate	Exact	
$\pi - 0.314159$	-0.0234db	-0.0238db	$+0.0004$db
$\pi - 0.1884955$	-0.0523	-0.0525	-0.0002
π	-0.1724	-0.1727	$+0.0003$
$\pi + 0.1884955$	-0.0523	-0.0525	$+0.0002$
$\pi + 0.219911$	-0.0418	-0.0421	$+0.0003$

case, from (26)

$$E_1 \cong 1 - \tfrac{1}{2} |E_2|^2 = 1 - \tfrac{1}{2}\left\{\frac{\sin\left[\sqrt{\left(\frac{\Delta\beta_*}{4\pi/c}\right)^2 + 1}\,\frac{2}{\pi}cz\right]}{\sqrt{\left(\frac{\Delta\beta_*}{4\pi/c}\right)^2 + 1}}\right\}^2 \tag{29}$$

and the loss has the form (just as in the case of sinusoidal coupling[3])

$$\left(\frac{\sin au}{u}\right)^2$$

which in our terminology has half-peak loss (with $\Delta\beta_*$ the variable) at

$$\Delta\beta_{*\frac{1}{2}}\,|_{\Delta\alpha=0} = \frac{1.8\pi}{z}. \tag{30}$$

For the numerical case of this paper, $z = 1000$ feet and

$$\Delta\beta_{*\frac{1}{2}}\,|_{\Delta\alpha=0} = 0.00565.$$

TABLE VI — PHASE ANGLE OF E_1 FOR $|\Delta\alpha/c| = 0$

$\Delta\beta\left(\frac{\lambda_m}{2}\right)$	Angle for E_1		Approximate −exact
	Approximate	Exact	
$\pi + 0.0015707963$	$-67.753°$	$-67.726°$	$-0.027°$
$\pi + 0.00314159264$	-47.111	-47.096	$-0.015°$
$\pi + 0.00471238891$	-30.086	-30.092	$+0.006°$
⋮			
$\pi + 0.0157079$	-9.085	-9.104	$+0.019°$

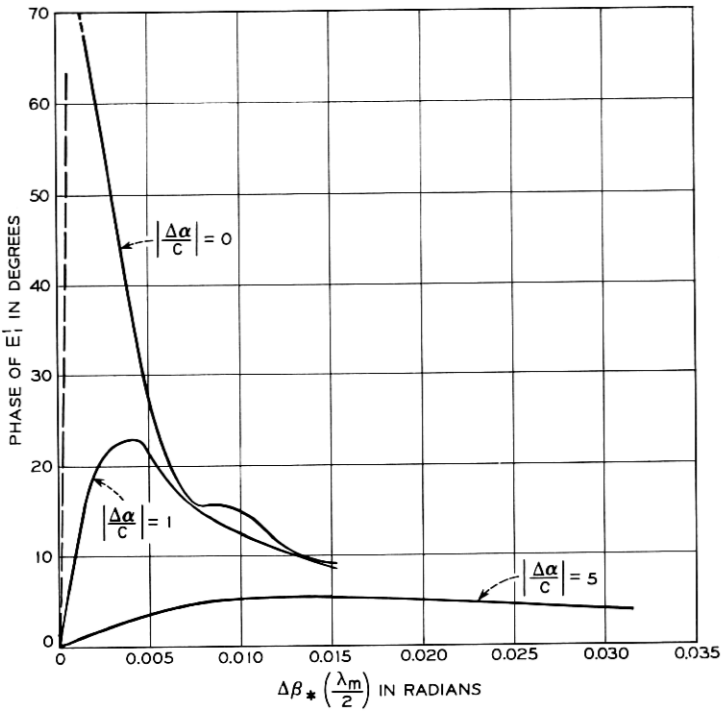

Fig. 8 — Phase of driven wave versus $\Delta\beta_*\lambda_m/2$ near $\Delta\beta\lambda_m = 2\pi$ for $|\Delta\alpha/c| = 0,1,5$.

In Table VII, the calculated value 0.0064 at $|\Delta\alpha/c| = 1$ is reasonable, since D. T. Young's[4] work based on the perturbation theory indicates that the true loss peak is the *convolution* of the shape for $|\Delta\alpha/c| \gg 1$ with the shape for $|\Delta\alpha/c| = 0$.

Consider now the peak loss at $\Delta\beta_* = 0$. When $|\Delta\alpha/c| \gg 1$, and $e^{\Delta\alpha z} \ll 1$, it can be shown that equation (9) simplifies to

$$E_1 | = e^{r_{3z}} \tag{31}$$

$$\left|\frac{\Delta\alpha}{c}\right| \gg 1$$

$$e^{\Delta\alpha z} \ll 1$$

$$\Delta\beta_* = 0$$

where

$$r_3 = -\frac{4}{\pi^2} c \left| \frac{c}{\Delta\alpha} \right| . \tag{32}$$

In Table VIII we compare the loss computed from (32) with the actual loss, and see that even for $| \Delta\alpha/c | = 1$ the error is only $\approx$30 percent. A consideration of the terms of equation (9) indicates that these errors would be approximately constant with increasing z.

A further simplification of the calculation of loss components now seems justified. For $| \Delta\alpha/c | \geqq 1$ it would appear that (31) and (32) can be used to calculate the peak loss due to a single square-wave coupling

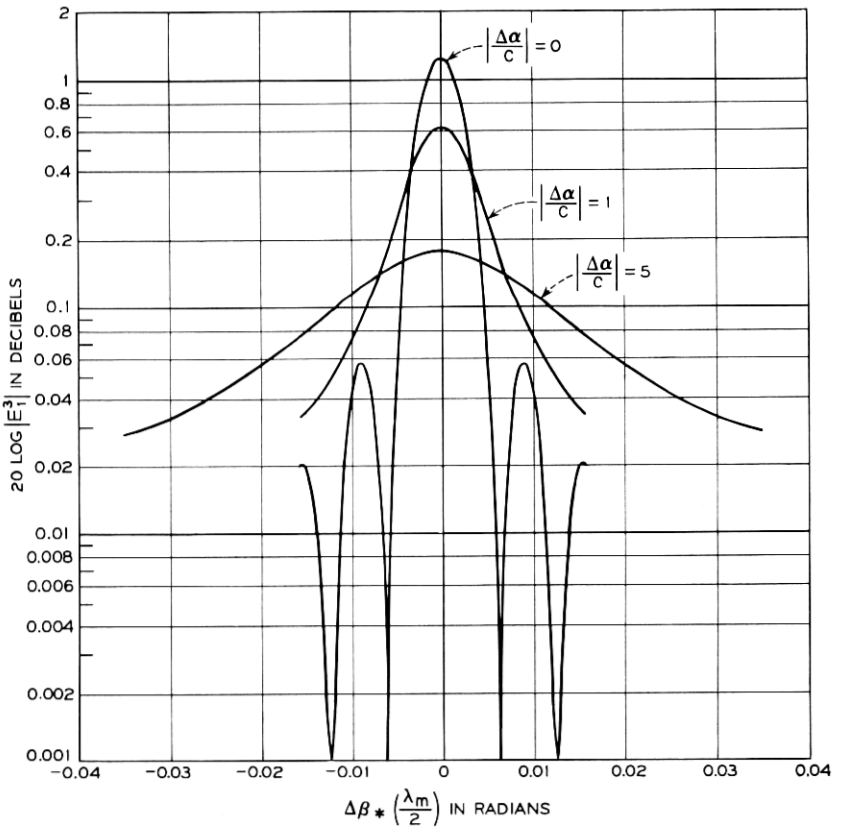

Fig. 9 — Driven-wave loss versus $\Delta\beta_*$ near $\Delta\beta\lambda_m = 6\pi$ (third harmonic) for $| \Delta\alpha/c | = 0,1,5$.

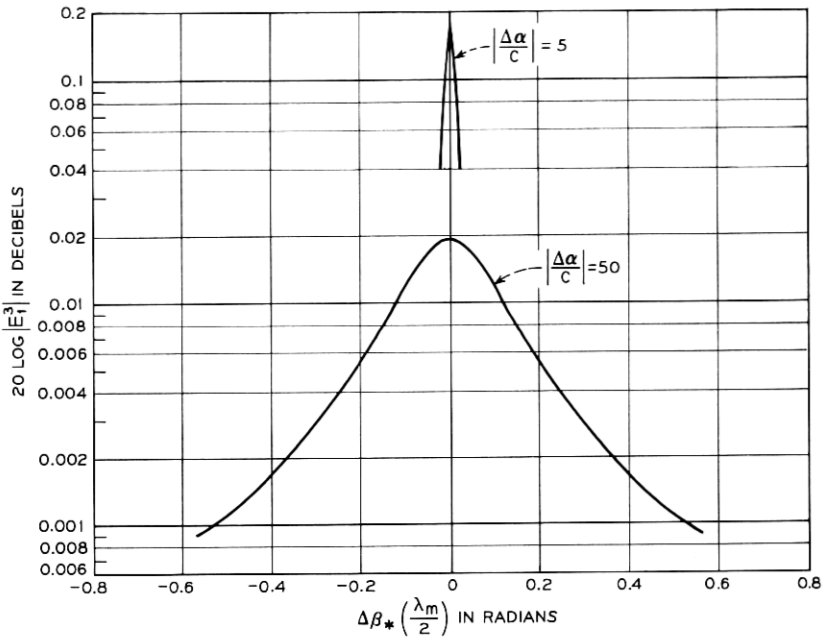

Fig. 10 — Driven-wave loss versus $\Delta\beta_*$ near $\Delta\beta\lambda_m = 6\pi$ (third harmonic) for $|\Delta\alpha/c| = 5,50$.

component. And the shape versus $\Delta\beta_*$ can be calculated from the work of D. T. Young, leading to an over-all attenuation defined by

$$|E_1| = e^{r_4 z} \tag{33}$$

where

$$r_4 = -\frac{4}{\pi^2} c \left|\frac{c}{\Delta\alpha}\right| \frac{1}{1 + \left(\frac{\Delta\beta_*}{\Delta\alpha}\right)^2} \tag{34}$$

in which we require z and $\Delta\alpha/c$ such that $e^{\Delta\alpha z} \ll 1$, $|\Delta\alpha/c| \geqq 1$.

TABLE VII — LIMITING AND TRUE VALUES

(1) $\left\|\frac{\Delta\alpha}{c}\right\|$	(2) Limiting value of $\Delta\beta_{*1/2}$ from equation (25)	(3) Calculated $\Delta\beta_{*1/2}$ from Figs. 6 and 7	Ratio of Col. (3) / Col. (2)
1	0.00493	0.0064	1.3
5	0.0246	0.0265	1.077
50	0.246	0.250	1.016

TABLE VIII — LOSS COMPARISON

$\Delta\beta_s = 0$		
$\left\lvert\frac{\Delta\alpha}{c}\right\rvert$	Loss (dB) from equation (32)	Actual loss (dB) equation (9)
1	− 8.68	− 6.57
5	− 1.74	− 1.62
50	− 0.1737	− 0.1727

ACKNOWLEDGEMENT

The author would like to acknowledge the contribution of Mrs. C. L. Beattie in programming the computer for the calculations given in Figs. 6 through 10.

APPENDIX A

Coupling Functions

We use the following equations to represent two coupled waves of amplitude E_1 and E_2:

$$\frac{d}{dz}E_1(z) = -\gamma_1 E_1 + c_{21}(z)E_2 \tag{35}$$

$$\frac{d}{dz}E_2(z) = c_{12}(z)E_1 - \gamma_2 E_2 \tag{36}$$

where $\gamma_n = \alpha_n + j\beta_n$ = complex propagation constant. Let

$$c_{21}(z) = jc_p e^{jk_c z}. \tag{37}$$

Energy conservation leads to:

$$c_{12}(z) = jc_p e^{-jk_c z}. \tag{38}$$

Also let

$$E_1 = e^{-\gamma_1 z} V_1 \tag{39}$$

$$E_2 = e^{-\gamma_2 z} V_2 . \tag{40}$$

Then (35) and (36) become:

$$\frac{dV_1}{dz} = jc_p V_2 e^{[\gamma_1 - \gamma_2 + jk_c]z} \tag{41}$$

$$\frac{dV_2}{dz} = jc_p V_1 e^{-[\gamma_1 - \gamma_2 + jk_c]z}. \tag{42}$$

We now see that the solution for $k_c = 0$ holds for k_c nonzero provided that we make the change

$$\Delta B = \beta_1 - \beta_2 + k_c$$

and put ΔB in place of $\Delta\beta = \beta_1 - \beta_2$ in the solution for $k_c = 0$.

Complete transfer of power between waves can occur when $\Delta B = 0$ or

$$k_c = (\beta_2 - \beta_1). \tag{43}$$

APPENDIX B

Square-Wave Coupling

We start with equations (1) through (4) representing uniformly coupled waves with $k_c = 0$ (see Fig. 1). Equations (9) through (14) with $c_* = c$ and $\Delta\beta_* = \Delta\beta$ give the amplitude of the output waves at z for the conditions $E_1 = 1.0$ and $E_2 = 0$ at $z = 0$. We apply these equations to the coupling distribution of Fig. 2 and find that the output amplitude for the undriven wave at $z = \lambda_m/2$ is:

$$E_2 \mid_{z=\lambda_m/2} = \exp\left[-j(\beta_1 + \beta_2)\frac{\lambda_m}{4}\right]\left\{\frac{+j\sin\left[\dfrac{c\lambda_m\sqrt{1+\left(\dfrac{\Delta\beta}{2c}\right)^2}}{2}\right]}{\sqrt{1+\left(\dfrac{\Delta\beta}{2c}\right)^2}}\right\}. \tag{44}$$

In the above, the simplification $\Delta\alpha = 0$ has been assumed.

Using the output waves at $z = \lambda_m/2$ as input conditions to the following coupling region (Fig. 2), the amplitude of the undriven wave at $z = \lambda_m$ is found to be:

$$E_2 \mid_{z=\lambda_m} = (-1)\frac{2\left(\dfrac{\Delta\beta}{2c}\right)}{\left[\left(\dfrac{\Delta\beta}{2c}\right)^2 + 1\right]} \cdot \sin^2\left[\frac{c\lambda_m}{2}\sqrt{1+\left(\frac{\Delta\beta}{2c}\right)^2}\right]\exp\left[-j\frac{(\beta_1+\beta_2)}{2}\lambda_m\right]. \tag{45}$$

The ratio of the undriven wave amplitude at $z = \lambda_m$ to the undriven wave amplitude at $z = \lambda_m/2$ is [from (44) and (45)]

$$\frac{E_2\,|_{\lambda_m}}{E_2\,|_{\lambda_m/2}} = j\,\frac{2\left(\frac{\Delta\beta}{2c}\right)}{\sqrt{1+\left(\frac{\Delta\beta}{2c}\right)^2}} \cdot \sin\left[\frac{c\lambda_m}{2}\sqrt{1+\left(\frac{\Delta\beta}{2c}\right)^2}\right] \exp\left[-j\,\frac{(\beta_1+\beta_2)}{4}\,\lambda_m\right]. \tag{46}$$

By imposing the condition

$$\frac{c\lambda_m}{2}\sqrt{1+\left(\frac{\Delta\beta}{2c}\right)^2} = \frac{\pi}{2} \tag{47}$$

we notice that the magnitude of (46) approaches two for $\Delta\beta \gg 2c$, that is, for very small coupling. Fig. 4 sketches the undriven wave amplitude as a function of z during the first two coupling intervals. We will now express the approximate or average coupling between the waves by using the linear approximation $E_2(z) = 2cz/\pi$. We notice that uniform coupling without phase reversal would have resulted in the relation $E_2(z) = cz$. We therefore arrive at the transformation

c (constant coupling) becomes

$2c/\pi$ (for periodically reversed coupling). (48)

The associated transformation of the condition for maxmium energy transfer, from (47), is

$$\Delta\beta\,|_{\text{maximum conversion}} = \frac{2\pi}{\lambda_m}\sqrt{1-\left(\frac{c\lambda_m}{\pi}\right)^2}. \tag{49}$$

We might notice here that the departure of the actual amplitude in Fig. 4 from the straight-line approximation, shown by ϵ in Fig. 4, has a maximum value which can be shown to be $0.21(c\lambda_m)/\pi$. Thus the deviation between our straight-line approximation and the actual amplitude becomes smaller for diminished values of coupling per unit λ_m.

We now specify c_* and $\Delta\beta_*$ in equations (9) through (14) to represent the waves with periodically reversed coupling using the average coupling approach. Since the in-phase build-up of power in the undriven wave is a maximum for $\Delta\beta$ specified by equation (49), we define a new differential phase parameter to give a departure from this condition:

$$\Delta\beta_* = \Delta\beta - \frac{2\pi}{\lambda_m}\sqrt{1-\left(\frac{c\lambda_m}{\pi}\right)^2}. \tag{50}$$

By comparison with equation (7), which represents an exact solution for complex coupling, this definition of $\Delta\beta_*$ seems reasonable. Numerical checks reported in the text verify this presumption. The value of c_* is given by (48).

It has already been noted, near equation (46) that two successive $\lambda_m/2$ coupling intervals give twice the undriven line amplitude compared with the first $\lambda_m/2$ interval, which is just what occurs for small constant coupling (no reversal) and $\Delta\beta = 0$. We also find that $\Delta\beta_*$ and c_* correctly give the wave amplitudes for periodically reversed coupling at z equal to integral multiples of $\lambda_m/2$, even when $\Delta\beta$ is not large compared with $2c$. For example, letting E_2 at $z = \lambda_m/2$ be 0.707 requires $(\Delta\beta/2c) = 1$ (see equation 44); we maintain equation (47) and (48) as before. Then, from (45), $| E_2 |$ becomes unity at $z = \lambda_m$ which is also predicted by $\Delta\beta_*$ and c_* in (9) through (14) and which is analogous to the behavior of two conventional 3 dB directional couplers in cascade.

The above discussion represents the changes in wave propagation introduced by coupling for $\Delta\beta$ in the vicinity of the value given by equation (49).

The perturbation solution[3] for *sinusoidal* periodic coupling is known to yield coupling absorption peaks when

$$\begin{aligned} \Delta\beta\lambda_m &= 2\pi p \\ p &= 1, 3, 5 \cdots . \end{aligned} \tag{51}$$

Similarly, there are other regions of strong interaction for the square-wave coupling of Fig. 2. For example, consider Fig. 5, which represents the situation when

$$\frac{kc\lambda_m}{2} = \frac{3\pi}{2}. \tag{52}$$

There is another region of $\Delta\beta$ defined by

$$\Delta\beta \,|_{\text{maximum conversion}} = 3 \cdot \frac{2\pi}{\lambda_m} \sqrt{1 - \left(\frac{c\lambda_m}{3\pi}\right)^2} \tag{53}$$

where there is a local maximum of conversion. As diagramed in Fig. 5, the average conversion coefficient is $2c/3\pi$. Thus the appropriate values of $\Delta\beta_*$ and c_* for equations (9) through (14) are

$$\begin{aligned} c_* &= \frac{2c}{3\pi} \\ \Delta\beta_* &= \Delta\beta - 3 \cdot \frac{2\pi}{\lambda_m} \sqrt{1 - \left(\frac{c\lambda_m}{3\pi}\right)^2}. \end{aligned} \tag{54}$$

More generally there are absorption peaks at

$$\Delta\beta_* = \Delta\beta - p\frac{2\pi}{\lambda_m}\sqrt{1 - \left(\frac{c\lambda_m}{p\pi}\right)^2} \tag{55}$$

$$c_* = \frac{2c}{p\pi} \tag{56}$$

where $p = 1, 3, 5, \ldots$

APPENDIX C

Sine Wave Coupling

We start with equations (1) and (2) with the coupling defined

$$c_{21} = c_{12} = jc \sin\left(\frac{2\pi z}{\lambda_m}\right). \tag{57}$$

Using perturbation theory[3], and letting $\Delta\alpha = 0$,

$$E_2' = c\int_0^z \sin\left(\frac{2\pi s}{\lambda_m}\right)e^{-j\Delta\beta s}\,ds \tag{58}$$

which yields

$$E_2 = \frac{c}{\left[\left(\frac{2\pi}{\lambda_m}\right)^2 - \Delta\beta^2\right]}\left\{\frac{2\pi}{\lambda_m} - e^{-j\Delta\beta z}\left[\frac{2\pi}{\lambda_m}\cos\left(\frac{2\pi z}{\lambda_m}\right) + j\Delta\beta\sin\left(\frac{2\pi z}{\lambda_m}\right)\right]\right\}. \tag{59}$$

Evaluating at $\Delta\beta = 2\pi/\lambda_m$ and $z = n\lambda_m/2$ yields

$$E_2\,|_{\Delta\beta = 2\pi/\lambda_m} = -j\frac{c}{2}\frac{n\lambda_m}{2} \tag{60}$$

with $n = 1, 2, 3. \ldots$

It can be verified that $\Delta\beta = 2\pi/\lambda_m$ yields the maximum value of E_2 at $z = n\lambda_m/2$.

Thus the equivalent uniform coupling value for sinusoidal coupling is

$$c_* = c/2 \tag{61}$$

which appears in Table I.

REFERENCES

1. Pierce, J. R., "Coupling of Modes of Propagation," J. Appl. Phys., *25* (February 1954), pp. 179–183.
2. Rowe, H. E. and Warters, W. D., "Transmission Deviations in Waveguide due to Mode Conversion: Theory and Experiment," presented at the Conference on Long Distance Transmission by Waveguide, January 29, 1959; Proc. IEE, *106,* Part B, Supplement 13 (1959).
3. Rowe, H. E. and Warters, W. D., "Transmission in Multimode Waveguide with Random Imperfections," B.S.T.J., *41,* No. 3 (May 1962), pp. 1031–1170.
4. Young, D. T., "Effect of Differential Loss on Approximate Solutions to the Coupled Line Equations," B.S.T.J., *42,* No. 6 (November 1963), pp. 2741–2794.
5. Rowe, H. E., "Approximate Solution for the Coupled Line Equations," B.S.T.J., *41,* No. 3 (May 1962), pp. 1001–1029.
6. Miller, S. E., "Coupled Wave Theory and Waveguide Applications," B.S.T.J., *33,* No. 3 (May 1954), pp. 661–719.